

Available online at www.sciencedirect.com**SciVerse ScienceDirect**

Energy Procedia 29 (2012) 594 – 605

Energy

Procedia

World Hydrogen Energy Conference 2012

Advanced Fuel Cell Development in Russia

Nikolai Sochugov^a, Thorsteinn I. Sigfusson^{a,b,c}, A.A. Solov'ev^a,
A.I. Kirdyashkin^a, V.D. Kitler^a, A.S. Maznoy^a and Yurii Tyurin^a

^a*Tomsk Polytechnic University, 652000 Tomsk, Russia*^b*University of Iceland, 101 Reykjavik, Iceland*^c*Innovation Center Iceland, 112 Reykjavik, Iceland*

Abstract

The paper reports scientific work performed at Tomsk Polytechnic University in Tomsk Russia and is a part of a larger project devoted to hydrogen technology. The aim of the work has been to develop Solid Oxide Fuel Cell membranes based on porous Ni-Al support and involving plasma technology for supplying the active substrate with active layers to be finally perfected with electron beam technology.

On the basis of this work it is hoped that a new and promising method has been developed with applications that will lead to lowering cost and increasing efficiency.

© 2012 Published by Elsevier Ltd. Selection and/or peer-review under responsibility of Canadian Hydrogen and Fuel Cell Association. Open access under [CC BY-NC-ND license](https://creativecommons.org/licenses/by-nc-nd/4.0/).

Keywords: Fuel cells; SOFC; Ni-Al; Electron Beam; Plasma.

Introduction

In the past two years considerable effort has been made to advance Russian fuel cell research and bring it to the forefront in the technology. This paper describes the results obtained in Tomsk Polytechnic University (TPU) in the process of developing new materials for fuel cells. As is known, the high cost of fuel cells is still a restrictive factor for the development of hydrogen power engineering. This is a reason for high importance of research aiming to develop new materials and technologies for fuel cells production.

Beam-plasma technologies are widely used to modify the surfaces of materials in a variety of fields of science and technology, however, their application in hydrogen power engineering is still far less than what is possible. To improve this, a new technology for the production of the track proton-exchange membrane based on polyvinylidene difluoride (PVDF) has been proposed by TPU. The structure of the porous membrane was formed through the irradiation of a PVDF polymer film in a cyclotron with argon

ions at the energy of 41 MeV followed by thermal processing and chemical etching. This particular and advanced method will be reported in detail in due course and is not subject of this paper.

Along with low-temperature fuel cells with a proton-exchange membrane, considerable attention in TPU is paid to developing solid oxide fuel cells (SOFC). Therefore, a more detailed examination will further be given to the application of beam-plasma technologies in the production of SOFCs on the metal bearing plate. These deserve higher interest for their reliability, resistance to thermocycling, and mechanical stability. Furthermore, the overall cost of the fuel cells can be significantly reduced by transition from the anode-supported construction to that with a porous metal plate performing the supporting function and the electrolyte and electrodes deposited as thin films.

At present, to manufacture metal components of SOFC such as porous plates, interconnectors and current collectors, as a rule, numerous types of ferrite stainless steel and alloys are used (e.g. AISI 446, 420, Inconel, Crofer, etc.) [1]. The mentioned stainless steels contain chrome within the range of 18 to 27 mass percent. As a result of long-term exploitation of these materials at operating temperatures of fuel cells ($\sim 800^{\circ}\text{C}$) chrome tends to diffuse towards the surface and be deposited as Cr_2O_3 on the anode or cathode surface, which makes it necessary to form conducting barrier layers on the metal plate/electrode borderline [2,3]. Chromium oxide decreases the catalytic activity of electrodes and, as a result, lowers the effectiveness of fuel cells. Intermetallic alloys based on nickel and aluminium, which are more resistant to oxidation at high temperatures [4], are prospective materials for producing the porous metallic base for fuel cells. Although extensive amount of information has been obtained about the resistance of bulk Ni-Al alloys and coatings to oxidation [5, 6], there are relatively few published works studying porous Ni-Al alloys. Only several works are devoted to investigating fuel cells based on porous Ni-Al alloys [7, 8].

Porous Ni-Al alloys are produced using methods of powder metallurgy [9, 10] as well as strain hardening of Ni-Al foam [7]. Powder technologies provide the possibility of sintering with layers of fuel cells as well as sintering of samples with different geometries. A prospective technique of producing porous Ni-Al alloys is the method of self-propagating high-temperature synthesis (SHS) [11]. The method is based on the effect of autothermal speeding-up of the heterogeneous reactions in the process of exothermic chemical transformation of the powder mix components into the target product. The SHS process is attractive due to its power efficiency, opportunity of providing unique characteristics of the structural and phase state as well as high functional properties of intermetallic and other materials. This paper concerns studying the possibility of manufacturing SOFCs on the metallic supporting plates based on a porous Ni-Al material using beam-plasma technologies as well as investigating its structure and electrochemical properties.

1. Research methods

The research has been focused on synthesizing the intermetallic alloy compound Ni+10%Al (here and throughout the paper the mass fraction of a substance is indicated) that has high strength and thermostability characteristics, catalytic activity [12], and a thermal coefficient of linear expansion (TCLE) close to TCLE of a deposited anode layer. The powders of Ni – UT- 4 (a purity of 99,9%, particles size of less than 20 μm), Al – ASD-6 (a purity of 99%, particles size of 5 μm), ALEX (a purity of 99% Al, 9% Al_2O_3 , average particles size of 100 nm) have been used as reaction components.

The prepared powder composition of Ni+10%Al has been molded into cylinder shaped prototypes with the diameter of 20 mm and height of 1 - 2 mm in a special press tool under the mechanical load from 50 to 280 MPa.

The process of self-propagating high-temperature synthesis (SHS) has been carried out according to the pattern shown in fig. 1 by means of heating of a prototype to the critical temperature of thermal explosion. The synthesis has been carried out in argon at pressure of 0.1 MPa. The prototype temperature was measured by a thermocouple BP5-BP20, the diameter of a junction is 100 μm ; the thermocouple signal has been recorded by the oscilloscope. For the purpose to stabilize the composition and material structure after the SHS, the prototypes have been exposed to annealing in a vacuum oven at temperature of 1100-1200 K and residual air pressure of 10^{-2} Pa during one hour.

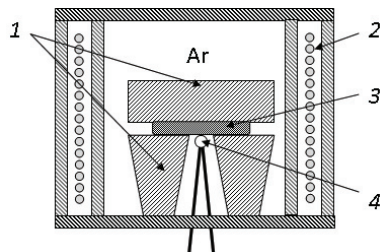


Figure 1. Scheme of experimental facility for SHS of Ni-Al substrates. 1 – steel cooling elements, 2 – resistance furnace, 3 – synthesized sample, 4 – thermocouple

The phase composition of the product has been defined by the method of an X-ray phase analysis using the X-ray diffractometer Shimadzu XRD 6000 and data bases «PDF4+». The chemical composition has been defined by the method of a micro X-ray spectral analysis using a Camebax Micro-Beam device. The thermal expansion coefficient study of the material has been carried out by the dilatometry method using the electronic dilatometer DIL 402 PC/4. The surface morphology study has been carried out using a Philips SEM 515 electronic scanning microscope. The porosity structure of the synthesis product has been studied by means of the metallographic analysis of a prototype flat cut using a microscope CarlZeiss «Axiovert 200 M-Mat», PA «ImageScope» and special stereometrical techniques [13]. Metallographic sections of the prototypes have been made using the method of embedding the prototypes into epoxy resin with the following polishing.

Gas permeability of Ni-Al substrates (related to nitrogen) has been studied using the in-house device made up of two sealed cavities being separated by the tested prototype. Each cavity has gas-intake pipes that let the force feed cavity be filled with nitrogen, and gas diffused into the measuring cavity be diverted. The amount of nitrogen passed through the prototype has been measured by the volumetric method (volume measurement of gas passed at constant pressure). The gas permeability G has been evaluated according to the following formula:

$$G = \frac{Q}{S\Delta P} \quad (1)$$

Where Q – gas flow ($\text{mole} \cdot \text{sec}^{-1}$), ΔP - pressure fall (Pa), S –prototype area (m^2).

The measurement of electrical resistance of transition Ni-Al/LSM cathode has been carried out according to a standard 4 probe scheme on measuring cells placed in the air at temperature of 700°C (fig. 2).

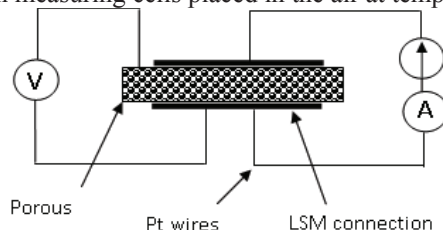


Figure 2. Scheme of measuring electric resistance of Ni-Al/LSM cathode transition.

For this purpose the cells with a LSM/Ni-Al/LSM structure have been made, where LSM = $\text{La}_{0.8}\text{Mn}_{0.2}\text{SrO}_3$ is a cathode material of SOFC. LSM layers with the size of $1\text{ cm} \times 1\text{ cm}$ have been formed on opposite sides of a Ni-Al prototype by depositing and drying a $\text{La}_{0.80}\text{Sr}_{0.20}\text{MnO}_3$ paste produced by NexTech Materials, Inc, US. While testing, direct current with the density of 0.5 A/cm^2 has been passed through a cell. The current and potential electrodes were supplied to the cell, and one of the potential electrodes was attached directly to the Ni-Al prototype by means of contact welding. This has been done for the purpose to measure the resistance of metal/LSM transition in the forward direction: (-)/Ni-Al/LSM/(+). Such electric polarity of the transition corresponds to the polarity transition of SOFC operation. The resistance value has been defined out of measurements of volt-ampere characteristics of the transition. It has allowed avoiding an error related to the presence of thermal e.m.f at the transition.

The formation of electrodes for SOFC on a supporting metal plate using conventional methods of high-temperature sintering is rather difficult since during the process of sintering an oxidizing medium may have a destructive impact on a metallic substrate, and a medium with low oxygen partial pressure leads to irreversible cathode decomposition. Therefore, for the anode layer sintering, nitrogen or hydrogen atmosphere has to be used. In this paper, the design/formation of fuel cells has been carried out in the following way. A layer of a $\text{NiO}(50\%)/\text{ZrO}_2\text{:Y}_2\text{O}_3(50\%)$ anode paste produced by ESL Electroscience has been applied over the Ni-Al substrate. The layer thickness is about $20\text{ }\mu\text{m}$. The anode layer sintering and its reduction have been carried out in the hydrogen atmosphere during two hours at temperature of 900°C . After that, a YSZ electrolyte film has been deposited on the anode layer by the method of $\text{Zr}_{0.86}\text{Y}_{0.14}$ target reactive magnetron sputtering.

The electrolyte layer thickness is $5\text{--}20\text{ }\mu\text{m}$ depending on the time of deposition (rate of film depositing is $4\text{ }\mu\text{m/h}$). The deposition of the YSZ electrolyte on substrates brought to temperature of 600°C has been carried out in an Ar/O_2 atmosphere at pressure of $0.2\text{--}0.3\text{ Pa}$. The pulse mode of magnetron operation has been used with the frequency of 50 kHz and discharge power of 1.5 kW . The process has been completed with the formation of the LSM cathode by depositing the $\text{La}_{0.80}\text{Sr}_{0.20}\text{MnO}_{3-x}$ paste produced by NexTech Materials, Inc., the USA. Electrochemical study of fuel cells on the Ni-Al base has been carried out using a ProboStatTM device (NorECs Norway) under the conditions described in detail in [14].

2. RESULTS AND DISCUSSION

2.1. Ni-Al substrate synthesis

In the investigations use has been made of the process of SHS of Ni-Al substrates in the mode of a thermal explosion which is running in the form of quick self-heating of a powder system from TE (explosion critical temperature) to TM (maximal temperature of explosive heating) within tR (chemical transformation time). In the system ASD-6/UT-4: TE = 790-850 K, TM = 1360-1460 K, tR = 0.8-1.3 sec, and in the system ALEX/UT-4: TE = 960-1020 K, TM = 1150-1250 K, tR = 3.2-4.5 sec. High values of TE and tR and low TM of the second system are conditioned by diffusive limits of the reaction rate, which apparently are bound with the presence of a considerable amount of aluminum oxide on the surface of ALEX aluminum particles.

The reaction product is a porous permeable material (fig. 3, a) consisting of composition phases Ni_3Al , NiAl , Ni . An average value of prototypes porosity depending on compacting pressure (PC) of a base mixture varies within 35-45%. The substrates produced practically in full repeat the geometry of initial powder prototypes. Vacuum annealing during one hour leads to diffusive homogenization and change in the phase composition of the material towards an equilibrium state [15]: quantity reduction of Ni , NiAl and an increase of Ni_3Al . Repeated annealing practically does not influence the composition. Morphology characteristics of phase components and material pores are also not changed under thermal treatment (fig. 4). However, after the first cycle of annealing the structure is stabilized.

According to the metallographic analysis of prototypes cut, it follows that depending on PC the diameter of gas-transport channels (DCan) and specific surface of substrates open pores (SSurf) of the composition ASD-6/UT-4 vary within DCan = 1 – 2 μm , SSurf = 200 - 500 mm^{-1} (fig.4a, dotted lines). After stabilizing annealing, the parameters are 20-50% changed (fig.4, a, full lines). Between the outer surfaces of substrates there is a space distribution of values DCan, SSurf (fig.4, b) conditioned

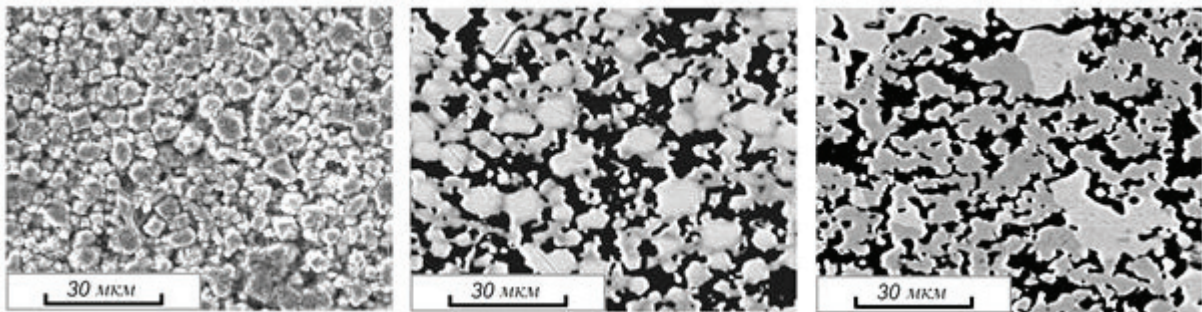


Figure 3. Ni-Al SHS substrates microstructure. Raster electronic microscopy. (a) - sample surface; (b),(c) - sample section surfaces before and after stabilizing sintering. Initial system ASD-6/UT-4.

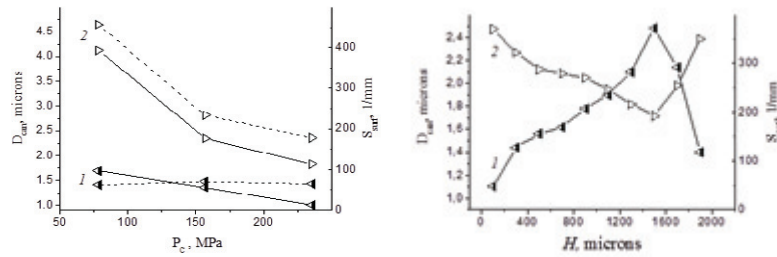


Figure 4. Porosity morphology parameters of Ni-Al SHS substrates. Curves 1 – DCan, curves 2 – SSurf. Part a – parameters depending on initial mixture compaction pressure; dotted lines – before stabilizing sintering, solid lines – after stabilizing sintering. Part b – morphology characteristics distributions in the longitudinal section of the sample; H – distance from the plate surface. Initial system ASD-6/UT-4. apparently by mixture pressing conditions and peculiarities of heat exchange of prototypes in the process of SHS.

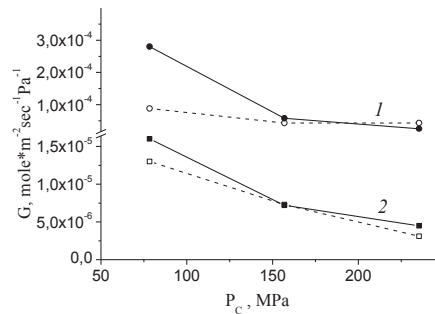


Figure 5. Gas permeability of Ni-Al samples obtained by SHS method depending on initial mixture compaction pressure. System ASD-6/UT-4 – curves 1, ALEX/UT-4 – curves 2. Dotted lines – before stabilizing sintering, solid lines – after stabilizing sintering.

Gas-transport properties of substrates produced are illustrated in fig. 5, showing that with the help of matching P_c and base mixture composition one can control the value of materials gas permeability within $G = 5 \cdot 10^{-6} - 3 \cdot 10^{-4}$ mole·m⁻²·sec⁻¹·Pa⁻¹. The measured values of the temperature coefficient of substrates linear expansion of composition ASD-6/UT-4 and ALEX/UT-4 are equal to $\alpha = 14 \cdot 10^{-6}$ K⁻¹ и $\alpha = 16.7 \cdot 10^{-6}$ K⁻¹ correspondingly (at 1073 K).

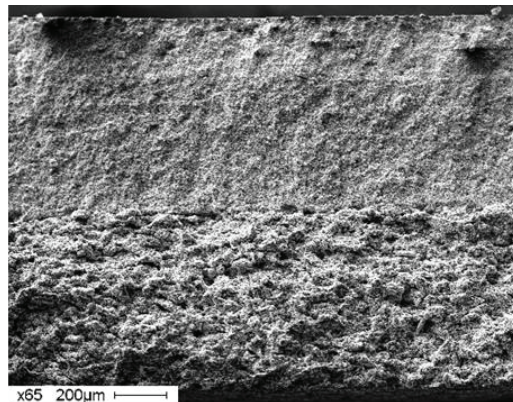


Figure 6. Cross-section of 3-layer Ni-Al sample with gradiently changing pore size.

In addition to this, the possibility to produce, using the SHS method, multilayer Ni-Al substrates with a gradient structure where the size of pores decreases along the prototype thickness towards the anode (fig. 6) has been demonstrated. For this purpose, each of the layers has been formed out of powders of various size. Thus, the most finely porous upper layer has been made using nanopowders, and the macroporous lower layer has been made using particles with an average size of $5\ \mu\text{m}$. The prototype production has been carried out by means of filling the mixture of the first layer into a press – form and it's leveling with a puncheon. Then the mixtures of the second and third layers have been put into. After that, the joint pressing of layers has been carried out. A macroporous layer is needed to supply fuel gas to the SOFC anode without considerable diffusive restrictions, and a finely porous layer is needed in the case if the anode layer deposited has small thickness (several μm).

2.2. Investigating oxidation resistance of Ni-Al substrates

The results of measuring the electric resistance of Ni-Al/LSM transition performed in the air atmosphere at 700°C are shown in Fig. 7. It can be seen that throughout the durability test the resistance grows, notably during the first 20 hours, when the growth rate is significantly higher than afterwards. This can be explained by the porosity of the contacting materials, which accounts for the oxide layer forming unevenly on the Ni-Al sample, this influencing the area of contact between the alloy and LSM.

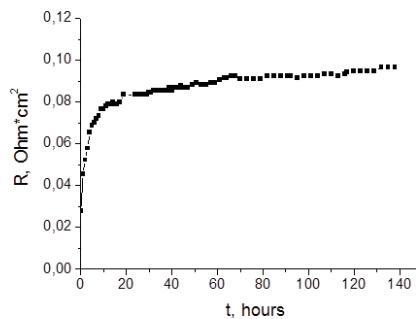


Figure 7. Dependence of the specific resistance of Ni-Al/LSM cathode transition on time under current density $0.5\ \text{A}/\text{cm}^2$ at temperature 700°C .

The slower increase of resistance after the first 20 hours is due to the slowdown in the growth of the oxide layer. On the linear part of the curve the resistance grows at the rate of $0.11 \text{ m}\Omega \cdot \text{cm}^2/\text{h}$, which is much slower than the similar parameter measured for 430L stainless steel ($3.3 \text{ m}\Omega \cdot \text{cm}^2/\text{h}$). Nevertheless, this is quite a high oxidation rate, considering that the required SOFC lifetime is 40000 hours. Therefore, for operating in the air it will be necessary to deposit protective coatings on the surface of the Ni-Al alloy. So, in [17] the coating of Mn-Co spinel on 08X18T1 stainless steel made in possible to lower the rate of resistivity growth to $0.026 \text{ m}\Omega \cdot \text{cm}^2/\text{h}$.

2.3. SOFC study on a bearing Ni-Al support

The cross-section image of a fuel cell is shown in fig. 8. An anode layer is of 20-35 μm thick and consists of rounded granules with the diameter of 1-3 μm . Since the size of anode granules is smaller than the size of pores on the surface of a Ni-Al layer, it makes provision for an anode layer be penetrated into the surface of a bearing substrate resulting in their strong bond with each other (the border between these two layers becomes hardly distinguishable).

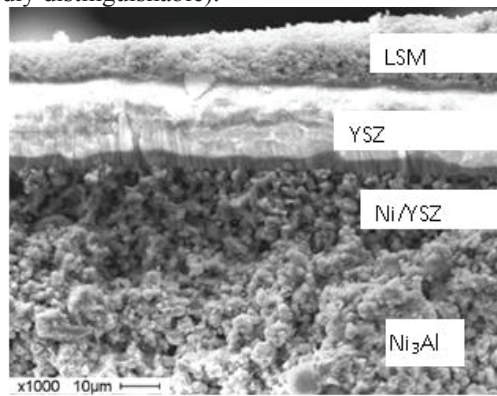


Figure 8. Cross-section of fuel cell with structure: Ni-Al SHS substrate – Ni/YSZ anode – YSZ electrolyte – LSM cathode (made after fuel cell examination). Scanning electron microscopy.

An YSZ electrolyte film formed on the anode layer initially has a columnar structure, and it can be explained by the prior film growth from granules tops of an Ni/YSZ anode. When the film thickness reaches 9 μm , the columnar growth stops, and a dense pore-free structure of the electrolyte is formed total thickness of which is 23 μm . A cathode layer of a fuel cell has the thickness of 10-20 μm and consists of granules with the size from 0.3 to 1 μm .

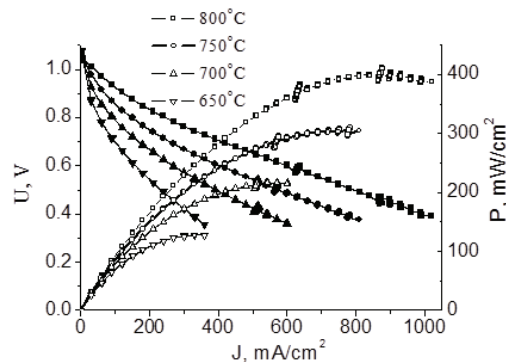


Figure 9. Current-voltage characteristics of fuel cell with Ni-Al SHS substrate. H_2 : 60 ml min^{-1} , air: 150 ml min^{-1} .

Voltage-current and power characteristics of a fuel cell produced are shown in fig. 9. The voltage of fuel cell idle running has been equal to 1.03-1.07 V depending on temperature that is very close to theoretically possible in the air and indicates gas impermeability of a YSZ electrolyte. Peak power density generated by a fuel cell is achieved at potential of 0.4-0.5 V and is equal to 120, 210, 300 and $400 \text{ mW}/\text{cm}^2$ at temperature from 650, 700, 750 and 800°C correspondingly. The similar power density at temperature of 800°C has been achieved using a fuel cell with a tubular metallic base and Ni-YSZ/YSZ/LSM structure [18]. The higher power density ($650\text{-}930 \text{ mW}/\text{cm}^2$) using fuel cells with a metallic support and an YSZ electrolyte has been achieved only when two-layer LSM/LSM-ScCeSZ cathodes [7], LSCF cathodes that have higher than LSM conductivity or cathodes containing noble metals [20] are utilized. The further improvement of fuel cell characteristics on a Ni-Al base support can be performed by depositing a Ni-YSZ anode with nanodimensional porosity using the method of magnetron sputtering, decreasing an YSZ electrolyte thickness up to $3\text{-}5 \mu\text{m}$, and making a cathode from a material of higher conductivity at temperature lower than 800°C , a $\text{La}_{0.6}\text{Sr}_{0.4}\text{Co}_{0.2}\text{Fe}_{0.8}\text{O}_3$ type.

It has been demonstrated before that the combination of an electron beam pretreatment of a thin YSZ sublayer (thickness of about $1\text{-}2 \mu\text{m}$) and magnetron sputtering lead to the formation of defect-free thin film YSZ electrolytes with a fine microstructure and a predominantly cubic crystal structure [21]. It is known that thin films deposited by magnetron sputtering have a columnar structure. By magnetron deposition of a YSZ electrolyte over the surface of a porous cathode, the growth of a film starts from the top of anode granules, which have the size of $0.5\text{-}3$ microns. Some columns of films near the bottom have the same diameter ($\sim 0.5\text{-}3$ microns). During the films growth, some columns merge forming a dense structure. The similar picture has been observed at the electrolyte formation shown in fig. 8. Therefore, to eliminate a columnar structure of an electrolyte film as well as to decrease its thickness keeping gas impermeability, it has been suggested expose a pre-deposited sub layer of an electrolyte to an electron beam with the following parameters: electrons energy - $10\text{-}12 \text{ keV}$, beam current - $\sim 15 \text{ kA}$, beam energy density - $E_s = 0.8 \text{ J}/\text{cm}^2$, pulse duration $2.5 \mu\text{sec}$.

The impact of an electron beam leads to the surface layer to be melted to the depth up to $1\text{-}1.5 \mu\text{m}$, and due to this its structure becomes more dense and its surface more smooth than the original anode surface. At depositing the second electrolyte layer, its formation stars from an almost smooth surface

rather than from granule tops of a porous substrate. Consequently, a dense and quite homogeneous structure is formed.

Thus, it becomes possible to form an YSZ electrolyte with a thickness of just 3-5 μm . Fig. 10 shows the X-ray diffraction patterns of YSZ films deposited on a porous anode substrate (a) and YSZ sublayer treated by an electron beam (b). In both cases, the cubic YSZ film phase has been generally detected. The cubic phase is the most preferable for the YSZ electrolyte, as it is responsible for high ionic conductivity of these films, and hence improves the performance of fuel cells. However, in the case of the film deposited on a porous anode substrate, in addition to the cubic phase of YSZ (YSZ-c) the diffraction patterns also have shown some amount of the tetragonal phase (YSZ-t). YSZ films with a cubic-tetragonal structure have also been reactively sputter-deposited by pulsed-DC magnetron sputtering in [22]. The YSZ electrolyte film deposited on a sublayer treated by an electron beam showed a predominantly cubic phase (Fig. 10, b).

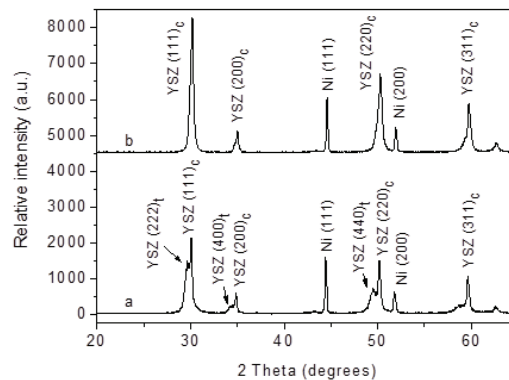


Figure 10. X-ray diffraction pattern of YSZ films deposited by magnetron sputtering without electron beam treatment (a) and with electron beam treatment of YSZ sublayer (b).

This effect could be due to the fact that in the process of an electron beam treatment a thin YSZ sublayer undergoes a rapid high temperature exposure, which results in the transformation of the tetragonal phase into the cubic phase. The results of X-ray analysis show that the pulsed electron-beam processing can replace the high-temperature annealing of films, which is traditionally used to improve the electrolyte structure and increase its gas tightness. This is particularly important in the manufacture of metal supported SOFCs because air atmosphere and high sintering temperatures (normally $> 1200^{\circ}\text{C}$) required for the densification of the electrolyte layer tend to lead to serious corrosion of the metallic substrate.

Additionally, our investigations have shown that the pulsed electron beam treatment of YSZ sublayers leads to the improvement of electrochemical parameters of anode supported SOFCs. In particular, an increase in values of cells power density has been observed. Fig. 11 shows the performances of two single cells that differ in ways of the YSZ electrolyte formation. In the first cell, the YSZ electrolyte with the thickness of 9 μm has been deposited by magnetron sputtering without an electron beam treatment, in the second cell, the electrolyte with the thickness of 3 μm has been deposited by using an electron beam treatment.

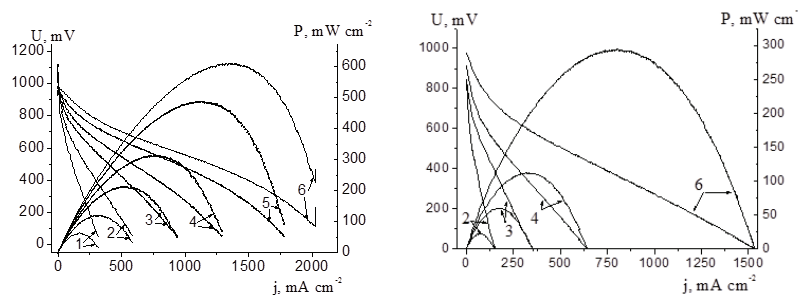


Figure 11. Current-voltage characteristics of single fuel cells with YSZ electrolyte deposited by magnetron sputtering without electron beam treatment (a) and with electron beam treatment of YSZ sublayer (b) at various temperatures (°C): 1 – 550; 2 – 600; 3 – 650; 4 – 700; 5 – 750; 6 – 800). H_2 : 40 ml min⁻¹, air: 150 ml min⁻¹.

The output power density of the second single cell reaches 620 mW/cm² at 800°C. This is almost twice as much as the value of the first fuel cell with an electrolyte, which has not been exposed to an electron beam treatment. The lower performance of the first cell is apparently associated with the lower conductivity of the magnetron sputtered electrolyte due to the presence of a tetragonal phase.

The results achieved give the ground to think that utilizing an electron beam treatment at the production of fuel cells on a bearing Ni-Al base support allows to substantially increasing the power generated by them.

Conclusion

As a result of the research performed, a technique for producing thin porous Ni-Al alloy plates using the SHS method with even or depth-gradient distribution of pores according to their size has been manifested. The porosity of the samples is 35-40%, while the width of the gas-transporting channels may vary from 1-2 to 10 and more μm depending on the initial powder size. It has been shown that this material is well combined with SOFC layers ($\alpha = 14 \cdot 10^{-6} \text{ K}^{-1}$) and has low oxidation rate in the air (0.11 m $\Omega \cdot \text{cm}^2/\text{h}$).

On a new Ni-Al base a fuel cell has been produced with the Ni-YSZ / YSZ / LSM structure, the electrolyte of which is formed by magnetron sputtering and which provides the power density of 400 mW/cm² at 800°C. A way of improving the microstructure and gas tightness of YSZ electrolyte deposited using magnetron sputtering by impulse electron beam treatment has been proposed. The research results prove the promising prospects for the development of Ni-Al materials by SHS to be used in solid oxide fuel cells at working temperatures of 650-800°C.

Acknowledgements

This work was supported by grant No. 11.G34.31.0003 (Leading Scientist T.I. Sigfusson). The complex investigation substrate properties were performed on the facilities of Tomsk Collective Access Centre for Material Study and Tomsk Scientific Centre SB RAS.

References

- [1] Wu J., Liu X. Recent Development of SOFC Metallic Interconnect // J. Mater. Sci. Technol., 2010, V. 26(4), p. 293-305.
- [2] Matus Y.B., De Jonghe L.C., Jacobson C.P., and Visco S.J. Metal-supported solid oxide fuel cell membranes for rapid thermal cycling // Solid State Ionics, 2005, V. 176, p. 443-449.
- [3] Choi J.-J., Lee J.-H., Park D.-S., Hahn B.-D., Yoon W.-H., Lin H.-T. Oxidation Resistance Coating of LSM and LSCF on SOFC Metallic Interconnects by the Aerosol Deposition Process // J. Am. Ceram. Soc., 2007, V. 90(6), p. 1926-1929.
- [4] Grabke H.J. Oxidation of NiAl and FeAl // Intermetallics, 1999, V.7, p. 1153-1158.
- [5] Wang Z., Tian W., Li X. Oxidation behavior of NiAl nanoparticles prepared by hydrogen plasma-metal reaction // Materials Chemistry and Physics, 2008, V.107(2/3), p. 381-384.
- [6] Kim S.H., Oh M.H., Kishida K., Hirano T., Wee D.M. Deposition of NiAl coating for improvement of oxidation resistance of cold-rolled Ni3Al foils // Intermetallics, 2005, V.13(2), p. 129-136.
- [7] Sadykov V.A., Usoltsev V.V., Fedorova Yu.E., Sobyanin V.A., Kalinin P.V., Arzhannikov A.V., Vlasov A.Yu., Korobeinikov M.V., Bryazgin A.A., Salanov A.N., Predtechenskii M.R., Bobrenok O.F., Ulikhin A.S., Uvarov N.F., Smorygo O.L., Il'yushchenko A.F., Ul'yanskii V.Yu., Zlobin S.B. Design of Medium-Temperature Solid Oxide Fuel Cells on Porous Supports of Deformation Strengthened Ni-Al Alloy // Russian Journal of Electrochemistry, 2011, V.47(4), p. 488-493.
- [8] Windes W.E., Smith C., Wendt D., Erickson A., Walraven J., Lessing P.A. Electrode coatings for high temperature hydrogen electrolysis // J. Mater. Sci., 2007, V.42, p. 2717-2723.
- [9] Morsi K., Fujii T., McShane H., McLean M. Control of heat generation during reaction synthesis // Scripta Materialia, 1999, V.40(3), p. 359-364.
- [10] Dong H.X., Jiang Y., He Y.H., Zou J., Xu N.P., Huang B.Y., Liu C.T., Liaw P.K. Oxidation behavior of porous NiAl prepared through reactive synthesis // Materials Chemistry and Physics, 2010, V.122, p. 417-423.
- [11] Merzhanov A.G. Tverdogorimennoe gorenie (Solid-flame Combustion) / A.G. Merzhanov, A.S. Mukasyan. – Moscow. : TORUS PRESS, 2007. – 336 p.
- [12] Naiborodenko Yu.S., Kasatsky N.G., Kitler V.D. et al. Katalizator i sposob polucheniya sintez-gaza uglekislotoy konversiey metana (Catalyst and Method for Producing Synthetic Gas by Carbon Dioxide Conversion of Methane). Patent RF No. 2349380, 2009. Bulletin No. 8.
- [13] Maznoy A.S., Kirdyashkin A.I., Maksimov Yu.M. Metodiki stereometricheskogo analiza morfologii poristyykh pronitsaemykh materialov (Methods for Stereometric Morphology Analysis of Porous Permeable Materials) // Izvestiya Vuzov. Poroshkovaya metallurgiya i funktsionalnyye pokrytiya (Proceedings of High Educational Institutions. Powder Metallurgy and Functional Coatings). – 2011. – Vol. 3. – p. 44-50.
- [14] Solovyov A.A., Sochugov N.S., Shipilova A.V., Yefimova K.B., Tumashevskaya A.Ye. Srednetemperaturnyye tverdooksidnyye toplivnyye elementy s tonkoplyonochnym ZrO₂:Y₂O₃ elektrolitom (Medium Temperature Solid Oxide Fuel Cells with Thin Film ZrO₂:Y₂O₃ Electrolyte) // Elektrokhimiya (Electrochemistry), 2011, Vol. 47(4), p. 524-533.
- [15] Diagrammy sostoyaniya dvoynykh metallicheskich sistem: v 3 t. (State Diagrams of Double Metallic Systems: In 3 Vol.) // [Edited by Acad. RAS N.P. Lyakishev] – Moscow.: Mashinostroeniye (Machine Building), 1996. – Vol.1 – 183 p.
- [16] Molin S., Kusz B., Gazda M., Jasinski P. Evaluation of porous 430L stainless steel for SOFC operation at intermediate temperatures // Journal of Power Sources, 2008, V.181, p. 31-37.
- [17] Bredikhin S.I., Zhokhov A.A., Frolova Ye.A., Ledukhovskaya N.V., Kuritsyna I.Ye., Sinitsyn V.V., Korovkin Ye.V. Zashchitnyye pokrytiya na osnove Mn-Co-shpineli dlya tokovykh kollektorov tverdooksidnykh toplivnykh elementov (Mn-Co-Spinel-Based Protective Coatings for Current Collectors of Solid Oxide Fuel Cells) // Elektrokhimiya (Electrochemistry), 2009, Vol.45, No5, p. 555-561.
- [18] Szabo P., Arnold J., Franco T., Gindrat M., Refke A., Zagst A., Ansar A. Progress in the Metal Supported Solid Oxide Fuel Cells and Stacks for APU // ECS Trans., 2009, V.25(2), p. 175-185.
- [19] Cho H.J., Park Y.M., Choi G.M. Enhanced power density of metal-supported solid oxide fuel cell with a two-step firing process // Solid State Ionics, 2011, V.192(1), p. 519-522.
- [20] Kong Y., Hua B., Pu J., Chi B., Jian L. A cost-effective process for fabrication of metal-supported solid oxide fuel cells // International journal of hydrogen energy, 2010, V.35, p. 4592 – 4596.
- [21] N.S. Sochugov, A.A. Soloviev, A.V. Shipilova and V.P. Rotshtain. An Ion-Plasma Technique for Formation of Anode-Supported Thin Electrolyte Films for IT-SOFC Applications // International Journal of Hydrogen Energy, 2011, V.36, Is.9, p. 5550-5556.
- [22] P. Briois, F. Lapostolle, V. Demange, E. Djurado, A. Billard // Surface & Coatings Technology, 2007, V.201, p. 6012-6018.